TEXTURE APPROXIMATIONS BY MODEL COMPONENTS

K. Helming

Institut für Metallkunde und Metallphysik, TU Clausthal, D-36678 Clausthal

1 Introduction

The texture (ODF) is traditionally calculated from pole figures, measured by x-ray or neutron diffraction. For cubic or hexagonal metals 3 - 4 pole figures are required for calculating the ODF. The angular resolution of 5° is normally sufficient to describe the most typical textures of deformed or recrystallized metals and alloys. Multi-phase materials like ceramics or rocks usually require large amounts of data (20 and more pole figures, resolution <5°) to calculate the complete ODF for each crystalline phase.

The amount of calculated or measured ODF data may be enormous. Nevertheless, large numbers of samples have to be compared with each other to find some relevant texture information about the texture modifying process. In these cases methods of texture approximation (or data reduction) working with model functions like spherical harmonics or Gaussian distributions are necessary. Furthermore suitable techniques of ODF description and presentation are necessary to reveal essential information. Methods are needed which permit determination of the amount and quality of information contained in available data sets and help to find efficient strategies of measurement. Starting from simple geometric considerations concerning directions and orientations, the presentation makes some proposals to solve these problems. Particularly the orientation distance is necessary to define model functions (texture components) or to construct a quasi-equidistant grid in orientation space. The latter can be used to approximate a texture (determined from pole figures) by huge number of fictitious crystallites. This kind of texture information can directly be used for numeric (grain by grain) simulations of texture-modifying processes.

2 Component Model

Texture approximation means, that the ODF will be presented by a small number of simple functions, which can be handled easily on a computer. This leads to a reduction of data without losing of texture information. Most propagation the series expansion with spherical harmonics has reached. They form an orthogonal system of basic functions. Mean values of anisotropic properties can be efficiently calculated by means of a small number of corresponding C-coefficients. This type of approximation is suitable to describe the ODF equally in the whole orientation space.

If the main features of the texture can be described by a few preferred orientations, the number of C-coefficients can be much larger as the number parameters which are re-

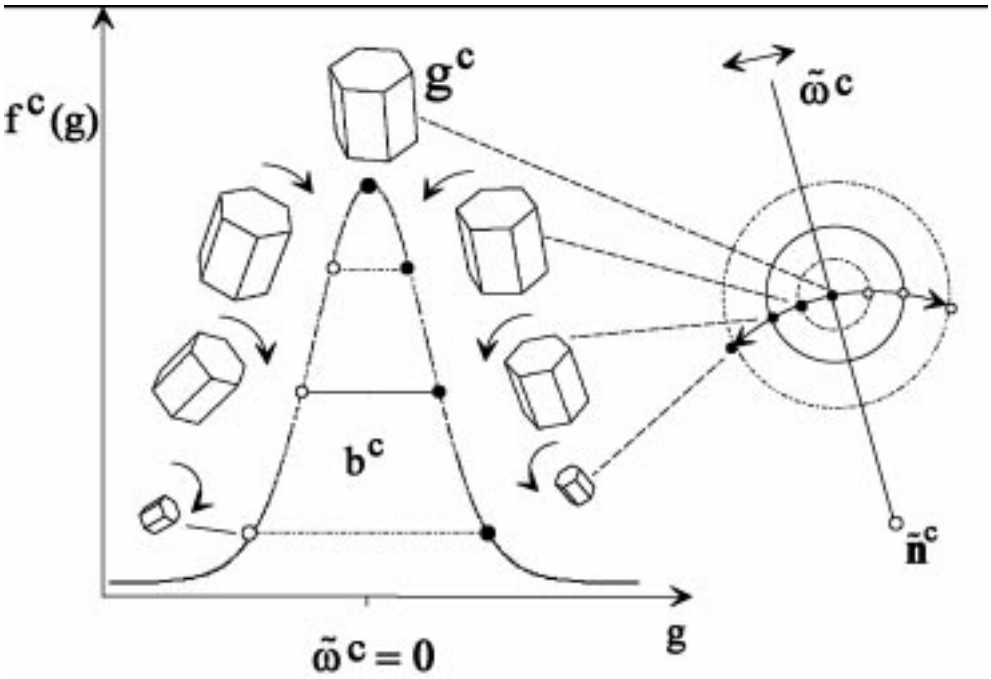

Figure 1 A Gaussian model function with a maximum at a preferred orientation g^c. $f^c(g)$ decreases with increasing . For a spherical component it not depends on the rotation axis $\tilde{n}$ that is chosen here perpendicular to the sheet of paper. The values of the function $f^c(g)$ can directly be interpreted as densities of volume fractions of similar oriented crystallites and are visualized by the volumes of unit cells (hexagonal crystal system) with corresponding orientations.

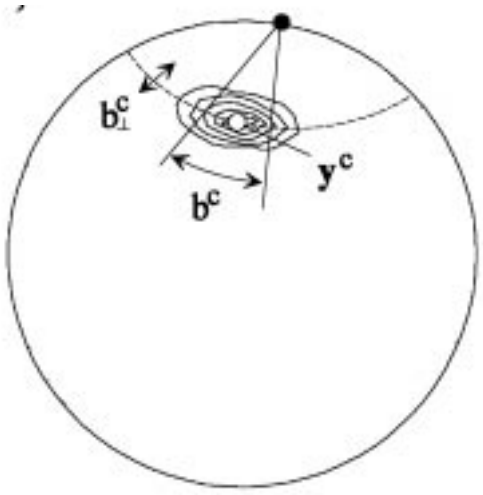

Figure 2 An elliptical component visible in a pole figure

ally required. In such cases the ODF-approximation by means of texture components

$$f(g) = F + \sum_c I^c f^c(g)$$
$$\text{with } F + \sum_c I^c = 1 \text{ and } \oint_G f^c(g)\, dg = 1 \tag{1}$$

should be preferred [1-6].

A component is described by a model function $f^c(g)$, which is locally restricted in the G-space, and an intensity I^c, which describes the volume fraction of all crystallites belonging to the component c. The quantity F gives the volume fraction of the crystallites, which are randomly oriented in the sample. It may be understood as the intensity of the only global (not restricted in the G-space) component used in the model. It is given by $f^0(g)=1$ for each $g \in G$. Because the model functions $f^c(g)$ are positive definite, the values can directly be interpreted as densities of volume fractions of similar oriented crystallites. To get a quantitative description of components [2] has defined a Gaussian distribution (cf. Fig.1)

$$f(g,g') = f(\tilde{\omega}) = N(\Psi)\exp[-(\tilde{\omega}/\Psi)^2]$$
$$\text{with } N(\Psi) \approx \frac{2\sqrt{\pi}}{\Psi\{1-\exp[-(\Psi/2)^2]\}} \tag{2}$$

where $\tilde{\omega}$ is the orientation distance between g and the maximum orientation g' of the distribution. $\tilde{\omega}$ is given by the orientation difference $\tilde{g} = g^{-1}g' = [\tilde{\omega}, \tilde{\boldsymbol{n}}]$ and can be calculated with

$$\cos\frac{\tilde{\omega}}{2} = \cos\frac{\varphi_1 - \varphi_1'}{2}\cos\frac{\varphi_2 - \varphi_2'}{2}\cos\frac{\Phi - \Phi'}{2} - \sin\frac{\varphi_1 - \varphi_1'}{2}\sin\frac{\varphi_2 - \varphi_2'}{2}\sin\frac{\Phi - \Phi'}{2} \tag{3}$$

if the orientations are given by Eulerian angles $(\varphi_1, \phi, \varphi_2)$.

Function (2) decreases with increasing $\tilde{\omega}$. Because it not depends on the rotation axis $\tilde{\boldsymbol{n}}$ turning g into g', it is called spherical (or peak) component. Considering the cyclic character of the G-space $\tilde{g} = [\pi - \tilde{\omega}, \tilde{\boldsymbol{n}}] = [\pi + \tilde{\omega}, -\tilde{\boldsymbol{n}}]$ relation $f = (\pi - \tilde{\omega}) = f(\pi + \tilde{\omega})$ should be valid. This condition is satisfied by the standard Gauss functions

$$f(\tilde{\omega}) = N(S)\exp[S\cos(\tilde{\omega})]$$
$$\text{with } S = \frac{\ln 2}{1 - \cos(b/2)}, N(S) = \frac{1}{I_0(S) - I_1(S)} \tag{4}$$

introduced by Matthies [5] where $I_n(x)$ are modified Bessel functions and b is the FWHM of the distribution. Beside a preferred orientation g' a component may be described by an additional preferred direction **f** referred to the sample coordinate system K_A. Such an elliptical component [6, cf. fig. 2] is given by

$$f(\tilde{\omega}) = N(S, S_f)\exp[S\cos(\tilde{\omega}) + S_f\cos(\tilde{\omega}_f)]$$
$$\text{with } \cos(\tilde{\omega}_f) = (g\,\boldsymbol{f})(g'\,\boldsymbol{f}),\ S_f = \frac{\ln 2}{1 - \cos(b_\perp/2)},$$
$$\text{and } N(S, S_f) = 1/\int_0^1 \exp(S_f t^2)(I_0(T) - I_1(T))dt \tag{5}$$
$$T = S_f(1 - t^2) + S$$

The corresponding pole figures are given by closed analytical expressions

$$P_h(y) = N(S, S_f)\exp(S\sin\frac{\vartheta^*}{2} + S_f\cos\vartheta_1\cos\vartheta_2)$$
$$I_0(S\cos\frac{\vartheta^*}{2} + S_f\sin\vartheta_1\sin\vartheta_2)$$
$$\text{with } \cos\vartheta^* = \boldsymbol{h}.(g'.\boldsymbol{y}),\ \cos\vartheta_1 = (g'.\boldsymbol{f}).\boldsymbol{h},\ \cos\vartheta_2 = \boldsymbol{f}.\boldsymbol{y} \tag{6}$$

allowing a simple numerical handling. Pole figures which are measured by diffraction can be understood as two-dimensional projections of the three-dimensional ODF:

$$\tilde{P}_h(\boldsymbol{y}) = \int_0^\pi [f(g_\varphi)]\, d\varphi = \frac{1}{2}[P_h(\boldsymbol{y}) + P_{-h}(\boldsymbol{y})] \tag{7}$$

Here $g_\varphi = g_{h \| y}$ with $0 \le \varphi \le \pi$ describes all orientations with their lattice plane normal **h** (ref. To K_B) lying parallel (or antiparallel) with the scattering vector **y**. The direction **y** is named sample direction, since it is related to the sample coordinate system K_A. Because of Friedel's law, pole figures are affected by an additional inversion center allowing only reduced pole figures, $\tilde{P}_h(y)$, to be measured. Especially for low crystal symmetries and multiphase systems Bragg-reflections of lattice planes may have the same or similar lattice distances

$$d^p_{(hkl)} = d^{p'}_{(h'k'l')},\ d^p_{(hkl)} \approx d^{p'}_{(h'k'l')} \tag{8}$$

causing total or partial coincidence. The pole figures measured by diffraction then read

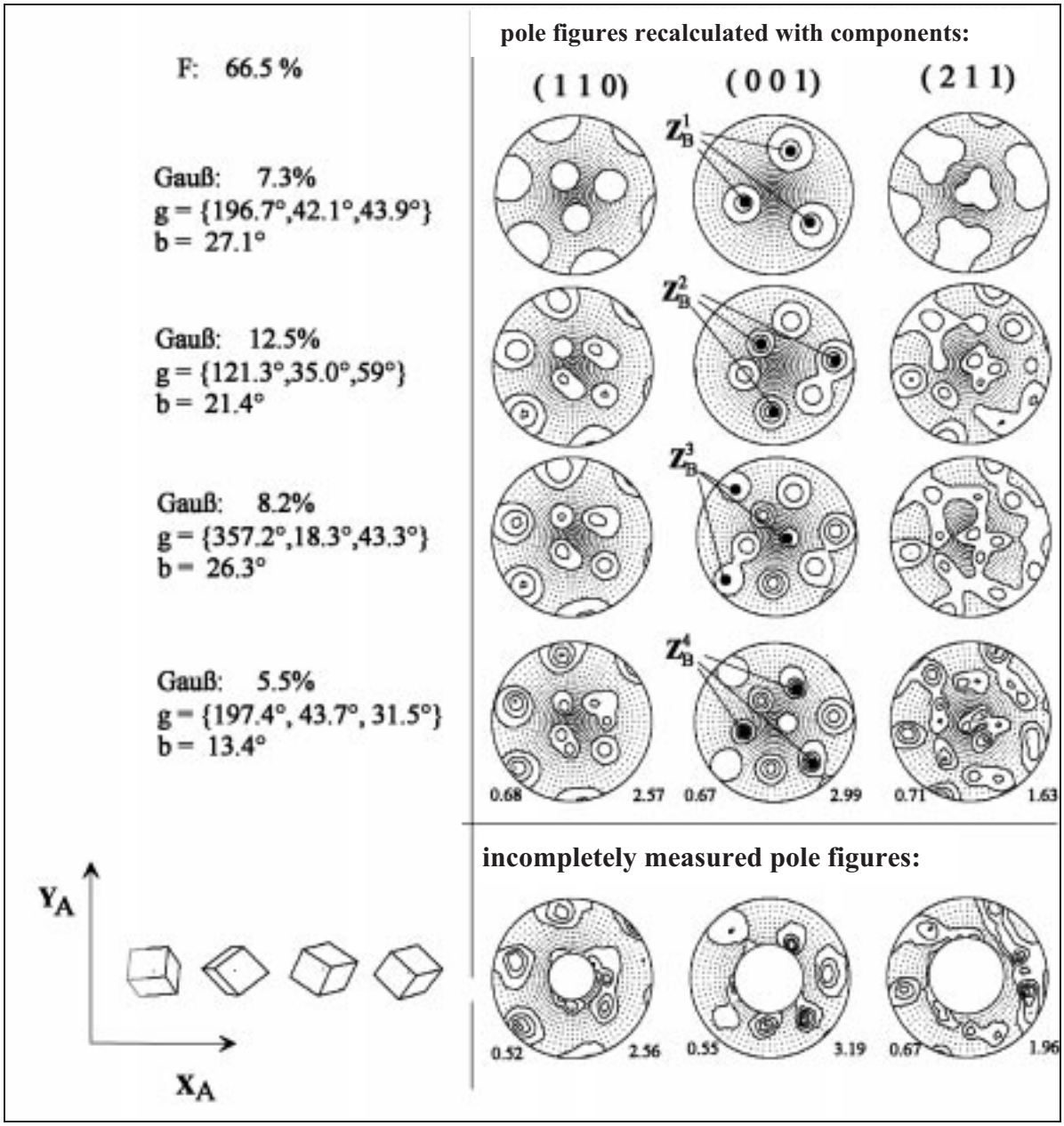

Figure 3 Texture components of a Fe/Ni-meteor given by F= 66.5% and four peak components. Bottom the pole figures incompletely measured by neutron diffraction are presented. Recalculated pole figures are shown for one (first row) up to four (fourth row) components which were calculated successively. The preferred orientations are presented by unit cells (bottom). Additionally the corresponding equivalent (100)||Z_B- directions are shown in the (100) pole figure.

$$\widetilde{D}_d(\boldsymbol{y}_r) = N_d \sum_{p,i} q_{id}^p \widetilde{P}_{\boldsymbol{h}_j}^p(\boldsymbol{y}_r) \qquad (9)$$

where *r* marks the sample directions *p* the crystalline phase and *i* the Miller indices *i≡(hkl)* of the measured pole figures, $\widetilde{D}_d(\boldsymbol{y}_r)$. The factors N_d and q_{id}^p depend on structure, phase fractions and absorption in a complex manner [7]. In the general case they must be treated as unknown parameters.

Now for each phase *p* a component description of the corresponding ODF, $f^p(g)$, is searched, trying to find the best fit of the experimental data $\widetilde{D}_d(\boldsymbol{y}_r)$ with the pole figures $\widetilde{D}_d^M(\boldsymbol{y}_r)$ which have been recalculated with the component model for all measured sample directions $\mathbf{y}_r$. The component parameters I^{pc}, g^{pc}, b^{pc}, $\boldsymbol{f}^{pc}$, $b_\perp^{pc}$ and the values N_d, q_{id}^p, can be determined by solving the least squares problem (w_{ir} are weight factors).

$$\sum_{i,r} w_{ir} [\widetilde{D}_d(y_r)] / N_d - \sum_{p,i} q_{id}^p \sum_c I^c \widetilde{P}_{\boldsymbol{h}_i}^M (g^{pc}, b^{pc}, \boldsymbol{f}^{pc}, b_\perp^{pc}, \boldsymbol{y}_r)]^2 \Rightarrow Min \qquad (10)$$

In order to determine the parameters by a non-linear algorithm, first estimates are necessary which may be obtained interactively from the graphical representation of the difference pole figures [8].

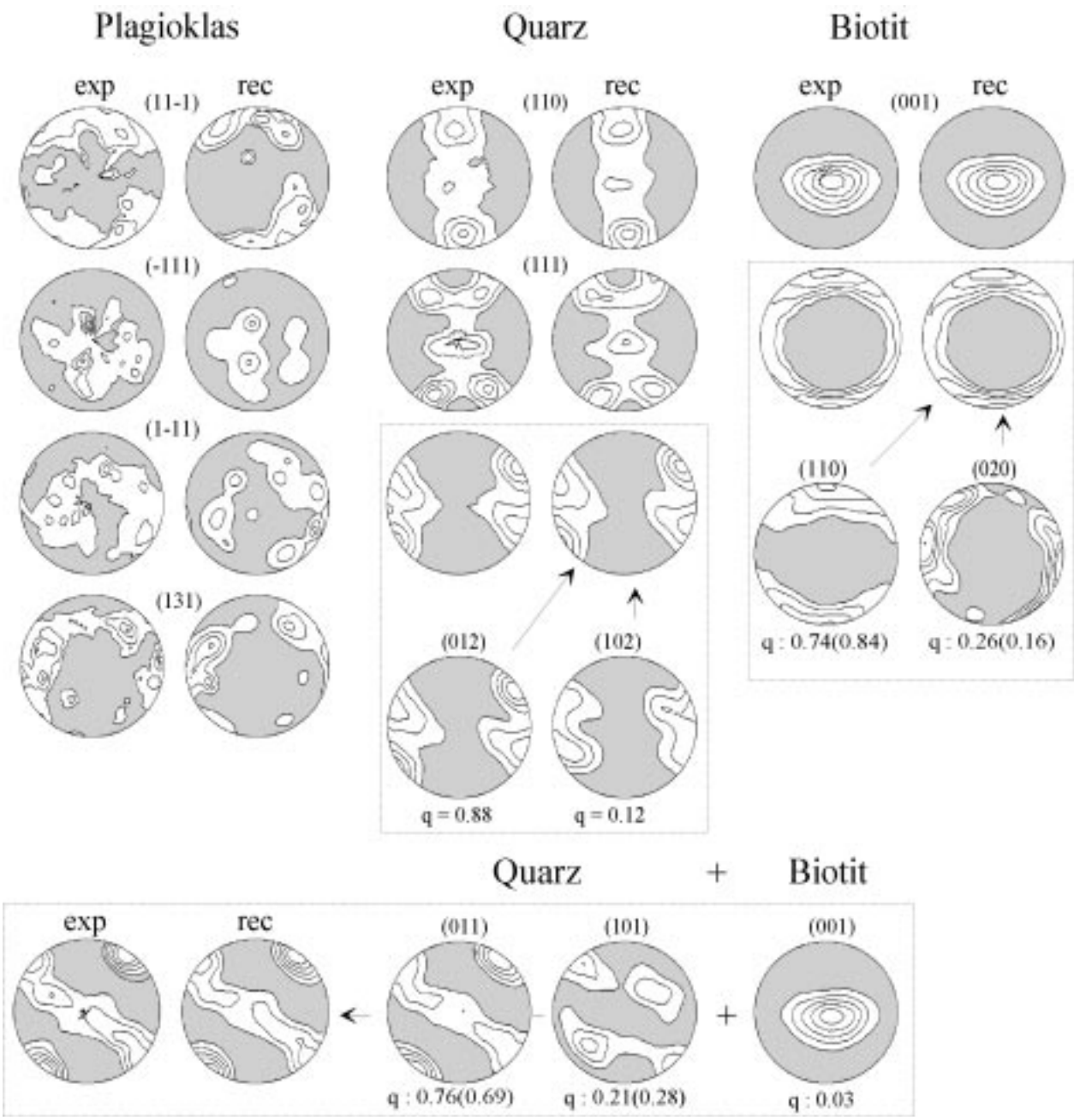

Figure 4 Ten measured and recalculated pole figures for quartz, biotite and plagioclase for a quartzite sample. The weak plagioclase texture is expressed with 12 components, the quartz texture with 8 and the biotite texture with 15. The values q_{id}^{p} refined by the component method are followed by brackets with corresponding values from structure calculations.

$$\Delta\widetilde{D}_d(\boldsymbol{y}_r) = \frac{\widetilde{D}_d(y_r) - \widetilde{D}_d^M(\boldsymbol{y}_r)}{N_d} \qquad (11)$$

on a PC-monitor. This iterative procedure is explained in more detail in [9]. Each iteration step contains

1. an interactive estimate of a small number of preferred orientation g^{pc}, $\mathbf{f}^{pc}$

2. the calculation of N_d, q_{id}^{p} and I^{pc} by linear approximation solving (10),

3. a refinement of g^{pc}, b^{pc}, $\boldsymbol{f}^{pc}$, $b_{\perp}^{pc}$ by non-linear approximation solving (10).

In fig. 3 the component determination based on three incompletely measured pole figures is shown [10]. Fig. 4 illustrates the application of the component method to a multi-phase system, a quartzite composed of triclinic plagioclase, monoclinic biotite and trigonal quartz. Because of the small number of pole figures and the low crystal symmetry, the texture of biotite can be considered as an estimate only [9].

The component description enables an efficient concentration of texture information. An solution for the ODF can be obtained which takes into account only the smallest necessary number of components. Estimates may be appropriate if the quality or quantity of measured data does not allow a precise calculation.

The approach to determine texture components requires that the number of available pole figures and the

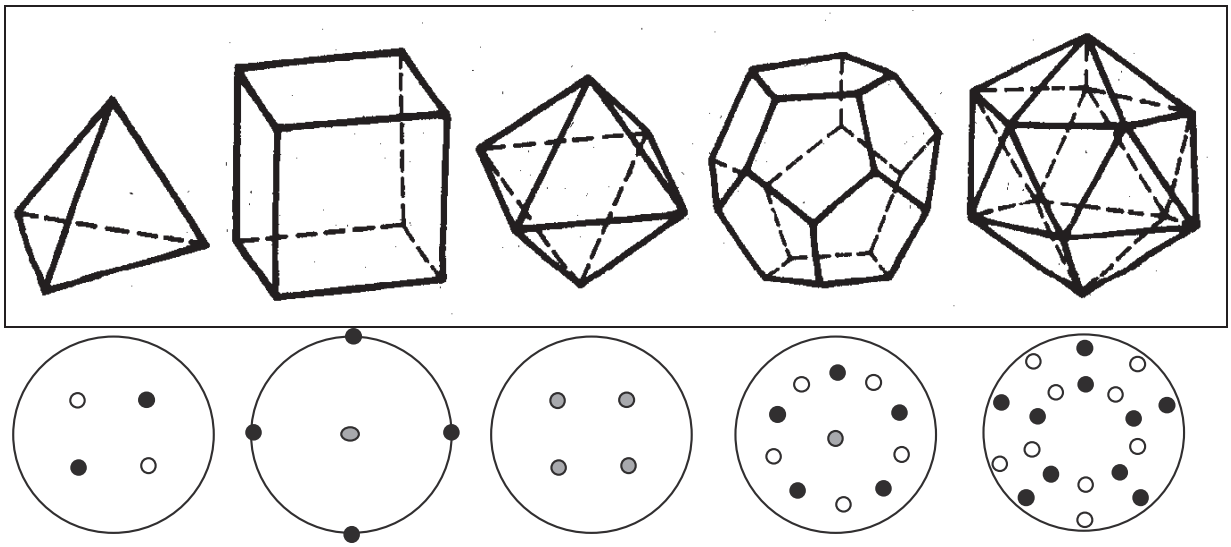

Figure 5 The five regular polyhedrons (top) and the normal directions of the facets (bottom). White directions (signed by white circles) show up, black ones show down, gray directions pointing on both, the upper and lower sphere. In each case every normal direction has the same number of next neighbours (3, 4 , 3, 5, 3 respectively). Furthermore the angular distance to the next neighbours is the same for each direction (109.74°, 90°, 70.51°, 63.45°, 41.81° respectively).

measured ranges are large enough such that any crystal orientation can be determined unambiguously. The least necessary amount of texture information in experimental pole figures only depends on crystal symmetry and the type of Miller indices of the diffracting lattice planes. The determination of minimal pole figure ranges (MPR) containing a minimum amount of texture information is explained in [11].

3 A nearly equal distant grid of orientations

Another possibility to determine texture components is based on a nearly equal distant (NED) grid of orientations, where he orientation distances to nearest neighbours as well as numbers of neighbours are nearly constant for each orientation [12]. The NED grid is characterised by only one parameter, its resolution Δ, which is the maximum distance between two nearest neighbour orientations. Unlike the presentation with Eulerian angles where $(\varphi_1, \Phi, \varphi_2)$ is decomposed into three successive rotations $[\varphi_2,\mathbf{Z}]$ $[\Phi,\mathbf{X}]$ $[\varphi_1,\mathbf{Z}]$ about the topical **Z**, **X** and **Z**-axis, now a split into two rotations is introduced by

$$g = [\vartheta, \boldsymbol{k}][\zeta, \boldsymbol{Z}_A] \quad \text{with } \vartheta = \angle(\boldsymbol{Z}_A, \boldsymbol{Z}_B),\ \boldsymbol{k} = \frac{\boldsymbol{Z}_A \times \boldsymbol{Z}_B}{\sin\vartheta} \tag{12}$$

The first (right) operator rotates K_A into K' through ζ on $\mathbf{Z}_A$. The second rotation turns K' into K_B by ϑ around the node direction **k**. ϑ is the angle (or angular distance) between $\mathbf{Z}_A = (\vartheta_A,\varphi_A)$ and $\mathbf{Z}_B = (\vartheta_B,\varphi_B)$

$$\cos\vartheta = \cos\vartheta_A \cos\vartheta_B + \cos(\varphi_B - \varphi_A)\sin\vartheta_A \sin\vartheta_B \tag{13}$$

After both operations K_A is identical with K_B. The orientation distance follows from (3)

$$\cos\frac{\omega}{2} = \cos\frac{\zeta}{2}\cos\frac{\vartheta}{2} \tag{14}$$

The rotation axis **n** lies in a plane with $(\mathbf{Z}_A+\mathbf{Z}_B)$ and $(\mathbf{Z}_A \mathrm{x} \mathbf{Z}_B)$

$$2\sin\frac{\omega}{2}\cos\frac{\vartheta}{2}\boldsymbol{n} = \sin\frac{\zeta}{2}(\boldsymbol{Z}_A + \boldsymbol{Z}_A) + \cos\frac{\zeta}{2}(\boldsymbol{Z}_A \times \boldsymbol{Z}_B) \tag{15}$$

To construct a NED grid of orientations one firstly needs a nearly equal-distant grid of directions. There are only five possibilities given by five regular polyhedrons (fig. 5) to construct an exact equal distant grid of directions. Based on the cube the resolution of the exact grid (Δ=90°) can be reduced introducing additional points in a systematic manner. The equal area projection of that kind of direction grid (ref. to K_B) is shown in fig. 6. On the cube face for x = *const* the directions shown are given by Cartesian coordinates

$$\boldsymbol{r}_y = \begin{pmatrix} x \\ y \\ z \end{pmatrix} = \frac{1}{N_{ij}} \begin{pmatrix} 1 \\ \tan(i\Delta) \\ \tan(j\Delta) \end{pmatrix} \text{ with } \mathrm{N_{ij}} = \sqrt{1 + \tan^2(i\Delta) + \tan^2(j\Delta)},\ -\tau < i, j \le \tau \tag{16}$$

where t = 90°/Δ must be an integer number. Δ is the maximum angle between nearest neighbour directions. It should be a divisor of 90°. In the same manner the directions for the remaining five cube facets can be built. The special arrangement of directions in the cube grid allows two-dimensional interpolations.

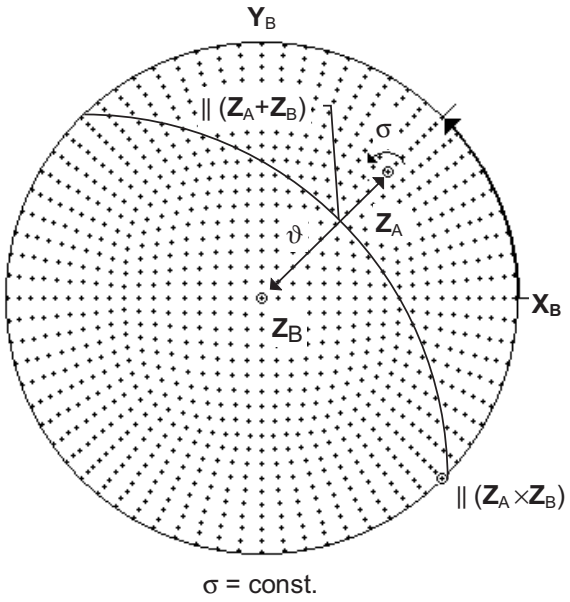

Figure 6 Equal area projection of a NED grid of directions ($\mathbf{Z}_A$ ref. to K_B) with $\Delta=5^o$. The rotation axis turning $\mathbf{Z}_A$ into $\mathbf{Z}_B$ is coplanar with ($\mathbf{Z}_A+\mathbf{Z}_B$) and ($\mathbf{Z}_A$ x $\mathbf{Z}_B$).

Two steps are necessary to create a NED grid of orientations. At first each direction in fig. 6 should be identified as a $\mathbf{Z}_A$ -axis (ref. to K_B). Secondly orientations with the same $\mathbf{Z}_A$-axis but different ξ (cf. (12)) are distinguished by different ξ-sections (cf. fig. 6). The partition of ξ (cf. (14)) is $\xi = 0, \Delta, 2\Delta, \ldots 360°-\Delta$ with Δ of the direction grid. Without any symmetry the total number T of single orientations $g'(0 \le t \le T)$ is

$$T = 4\tau(6\tau^2 + 2) \qquad (17)$$

since the number of ξ-values for $\mathbf{Z}_A$ -axis is 4τ and the number of directions on the cube is $6\tau^2+2$ (six faces with τ^2 points and two remaining edges). For $\Delta = 5°$ ($\tau = 18$) only 140112 orientations are necessary unlike a 5°-partition based on the Eulerian angles φ_1,Φ,φ_2 with 181476 orientations. Since K_B and not K_A is the reference system (fig. 6), an existing crystal symmetry can be used to reduce T in a simple manner. In the case of cubic symmetry one gets T = 5838 ($\Delta = 5°$), because only the 24th part of a cube surface has to be considered. If $\mathbf{Z}_A$-axis is parallel to an n-fold symmetry axis of the crystallite the range of ξ is reduced to $0 < \xi \le 360°/n$.

If the preferred orientations of the components in (10) are given by the single orientations of a NED grid and the half widths for all components are equal to the resolution Δ only the intensities/volume fractions must be calculated. This simply requires a linear algorithm (I-fit) that can be performed automatically, i.e. it works independently of the

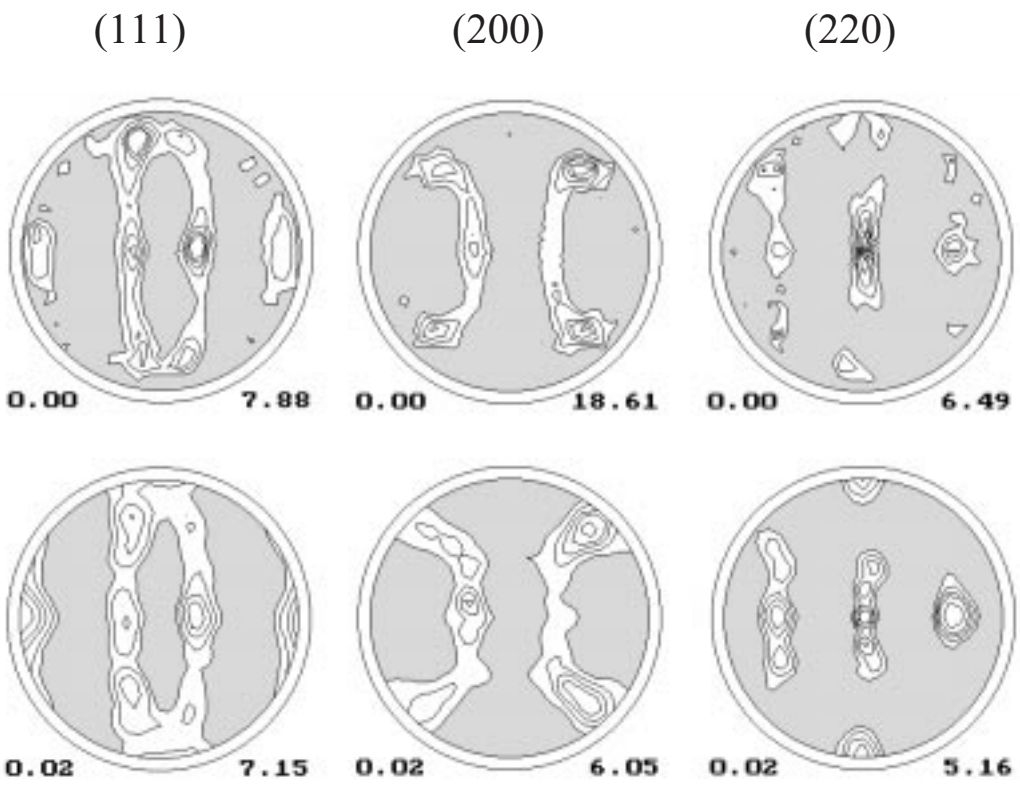

Figure 7 Measured (top) and recalculated (bottom) PFs of extruded Al. Using NED components with $\Delta = 15°$ (T = 218) the I-fit yields 37 remarkable components.

user. If the *I*-fit results in some components with negative intensities, the solution should be considered as a first estimate of an iterative algorithm. Negative or small intensities may be caused e.g. by errors of measurement. The corresponding components should be deleted before the next iteration step, i.e. before repeating the I-fit. Fig. 6 shows three measured and recalculated PFs of extruded Al [13]. Using NED components with D = 15° (T = 218) the I-fit yields 37 components after five steps.

4 Conclusions

The description of textures by means of a small numbers of components (preferred orientations) is an extraordinarily concise method. It may reveal relevant information about the texture modifying process even in those cases where the texture information contained in the measured pole figures is rather limited. ODF-calculations are possible for multi-phase materials like rocks or multilayers, where Bragg reflections often coincide. Component orientations and half widths are usually be calculated by applying non-linear iterative algorithms. For this first estimates are necessary which can be obtained interactively from the graphical representation of the diffraction data. This interactive modus of the component fit leads to a large reduction of data without losing of relevant texture information.

The automatic modus of the component fit avoids the disadvantage of the extensive interactive search for preferred orientations. On the other hand the disadvantage of a large number of (initial) NED components must be accepted. The set of components obtained can be interpreted as an ensemble of single orientations representing the texture. The intensities of the components may be assumed as volumes of pseudo crystallites with NED orientations. This type of texture approximation can directly be used for numeric simulations of texture modifying processes, like Taylor model or relaxed constraints.

Literature

1. G. Wassermann, Texturen metallischer Werkstoffe, Springer Verlag 1939; G Wassermann and J. Grewen. Texturen metallischer Werkstoffe, Springer Verlag. 1962
2. H.J. Bunge, Mathematische Methoden der Texturanalyse, Berlin, Akademie-Verlag.1969
3. W. Truszkowski, J. Pospiech, J. Jura und B. Major. In Proc. 3e Colloque Européen sur les Textures de Deformation et de Recristallisation des Metaux et leurs Applications Industrielles (Ed. R. Penelle), Pont-a-Mousson (1973), 235-257.
4. K. Lücke, J. Pospiech, J. Jura and J. Hirsch. *Z. Metallkd.* **77**, (1986) 312-321.
5. S. Matthies, G.W. Vinel and K. Helming Standard Distributions in Texture Analysis. Vol I-III, Akademie-Verlag Berlin. (1987-90).
6. K. Helming, K. Texturapproximation durch Modellkomponenten. Habilitation Thesis, TU Clausthal. 1995
7. H.J. Bunge, M. Dahms, and H.G. Brokmeier, H.G. The determination of the integrated intensities from polycrystalline samples with preferred orientations. *Cryst. Rev*. **2**, (1989) 67-88.
8. K. Helming and T. Eschner *Cryst. Res. Technol*. **25**,(1990) K203-K208.
9. K. Helming, *Physics of the Solid Earth*, engl. translation: Vol. **29**, (1994) No. 6, 523-532; russ. edition (1993), 73-82.
10. K. Helming,, H.-R. Wenk, C.S. Choi and W. Schäfer (1994a). In: H.J. Bunge, S. Siegesmund, W. Skrotzki, K. Weber (Eds): Textures of Geological Materials. DGM Press, 303-326.
11. K. Helming, Minimal pole figure ranges for quantitative texture analysis, *Textures and Microstructures* **19**,(1992) 45-54.
12. K. Helming,: A nearly equal distant grid of orientations for quantitative texture analysis. *Textures and Microstructures* **28** (1997), 219-230.
13. B. Fels. Textur- und Mikrostrukturuntersuchungen an stranggepreßten Aluminum, Diplom Thesis, TU Dresden. (1996)

Texture components were introduced by Wassermann [] to characterize different classes of textures by a few numbers of ideal orientations, given by ideal orientations and a corresponding spread. Here you see two pole figures of rolled iron which can be explained by three preferred orientations. The orientation parameter were directly deduced from the pole figures, i.e. for the Goss-orientation (100)[110] given by the sign đ the normal of (100) is parallel to the normal direction of the sheet and the lattice direction [110] is parallel to the polling direction WR. The orientational spread was estimated from the contour lines of the pole figures.